MOLECULAR & CELLULAR TOXICOLOGY, Vol. 2, No. 1, 21-28, March 2006

Hepatic Gene Expression Analysis of Gadolinium Chloride Treated Mice

Sun-Young Jeong[1,2], Jung-Sun Lim[2], Ji-Yoon Hwang[2], Yong-Bum Kim[1,2], Chul-Tae Kim[3], Nam-Seob Lee[3] & Seokjoo Yoon[1,2]

[1]Department of Biopotency/Toxicology Evaluation, University of Science & Technology, Daejeon, Korea
[2]Korea Institute of Toxicology, KRICT, P.O. Box 123, Yuseong, Daejeon, Korea
[3]Department of Anatomy, College of Medicine, Konyang University, Nonsan, Korea
Correspondence and request for materials should be addressed to S. Yoon (sjyoon@kitox.re.kr)

Accepted 15 February 2006

Abstract

Gadolinium chloride ($GdCl_3$) was known to block Kupffer cells and generally its toxicity study based on blocking these cells. Therefore, $GdCl_3$ frequently used to study toxic mechanisms of hepatotoxicants inducing injury through Kupffer cells. We also tried to investigate the effect of $GdCl_3$ on CCl_4 toxicity, typical hepatotoxicants. Administration of $GdCl_3$ to mice significantly suppressed AST (asparatate amino transferase), ALT (alanine amino transferase) levels which were increased by CCl_4 treatment. However, $GdCl_3$ didn't inhibit the phagocytotic activity of Kupffer cells. Malondialdehyde (MDA) is a good indicator of the degree of lipid peroxidation. In this study, MDA increased by $GdCl_3$ administration not by CCl_4. To understand the toxicity of $GdCl_3$, we analyzed global gene expression profile of mice liver after acute $GdCl_3$ injection. Four hundred fifty two genes were differentially expressed with more than 2-fold in at least one time point among 3 hr, 6 hr, and 24 hr. Several genes involved in fibrogenesis regulation. Several types of pro-collagens (Col1a2, Col5a2, Col6a3, and Col13a1) and tissue inhibitor of metalloproteinase1 (TIMP1) were up regulated during all the time points. Genes related to growth factors, chemokines, and oxidative stress, which were known to control fibrogenesis, were significantly changed. In addition, $GdCl_3$ induced abnormal regulation between lipid synthesis and degradation related genes. These data will provide the information about influence of $GdCl_3$ to hepatotoxicity.

Keywords: Gadolinium chloride ($GdCl_3$), Fibrogenesis, Hepatic gene expression

Gadolinium chloride ($GdCl_3$), a rare earth metal, has been frequently used to block the activity of Kupffer cells in *in vivo* models[1]. Kupffer cell, the resident macrophage of the liver, has been linked to a pathological role in liver injury induced by hepatotoxicants, such as carbon tetrachloride (CCl_4). When activated, Kupffer cells can synthesize and release a variety of immunomodulating and inflammatory mediators capable of causing hepatic injury, such as oxygen-derived free radicals, nitric oxide, lipid mediators, and cytokines. However, inhibition of Kupffer cells with $GdCl_3$ prevented acute or chronic liver damage induced by CCl_4[2-5]. *In vivo* experiment, treatment with $GdCl_3$ prevented CCl_4-induced increase in transforming growth factor-beta (TGF-β) expression that stimulate production of collagen in stellate cells[5]. Moreover, treatment with $GdCl_3$ prevented malondialdehyde (MDA), a good indicator of the lipid peroxidation which is one of CCl_4-induced liver injury mechanism[2-4]. However, despite this interest it is not clear whether $GdCl_3$ actually cause depletion of Kupffer cells or not. Cynthia, J. *et al.* demonstrated that treatment with $GdCl_3$ didn't inhibit the phagocytotic activity of Kupffer cells[6]. Furthermore, there is not enough information on the toxicity of $GdCl_3$. $GdCl_3$ is known to inhibit the function of the mononuclear phagocytic system, induce mineralization in the liver and have an anticoagulant effect by inhibiting clotting reactions[7]. This study is, therefore, designed to investigate as follows; i) the effect of acute dose of $GdCl_3$ on the Kupffer cell and liver and ii) the effect of $GdCl_3$ on CCl_4-induced injury. In this study, we investigated gene expression by using microarray technique.

Effect of $GdCl_3$ Pretreatment on CCl_4-induced Hepatotoxicity

Injury to the liver, whether acute or chronic, eventually results in an increase in serum concentrations of aminotransferases. Aminotransferases are highly concentrated in the liver. AST is also diffusely represented in the heart, skeletal muscle, kidneys, brain, and red blood cells, and ALT has low concentrations in skeletal muscle and kidney[8]; an increase in ALT

serum levels is, therefore, more specific factor for liver damage. In this study, ALT level shown more changeable than AST level did. At 3 hr, the level of AST and ALT after $GdCl_3$ treatment significantly increased (AST: 66.00±14.73, ALT: 65.00±18.08). Increased AST and ALT levels were recovered at 24 hr in a dose dependent manner (AST: 52.67±1.53, ALT: 18.67±6.81). At 24 hr after CCl_4 treatment, the level of AST and ALT significantly increased (AST: 83.00±11.53, ALT: 125.00±46.68). At same time, co-treatment of mice with $GdCl_3$ and CCl_4 didn't show increases in AST and ALT (AST: 55.33±1.53, ALT: 36.33±4.16) (Fig. 1).

Histopathological evaluation of liver animals treated with $GdCl_3$ at all time points showed minimal subcapsular inflammation and necrosis. Based on biochemical data (Fig. 1), we expected co-treatment of mice with $GdCl_3$ and CCl_4 would prevent CCl_4 induced toxicity. However, at 24 hr after treatment, in both group showed minimal and mild subcapsular inflammation and necrosis (Fig. 2).

Phagocytotic activity in liver was determined by uptake of carbon particles. Pretreatment of mice with $GdCl_3$ didn't inhibit phagocytotic activity at all con-

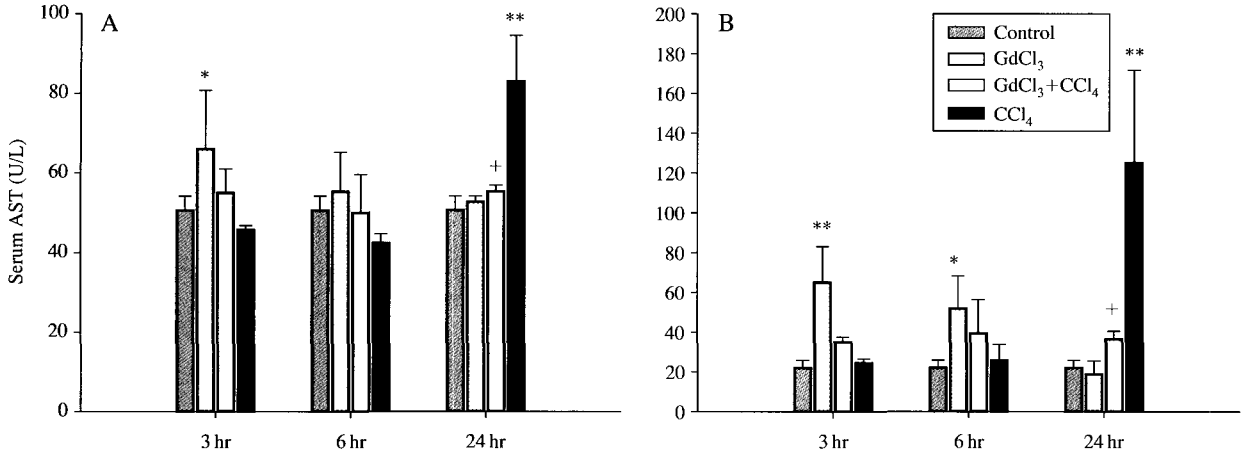

Fig. 1. (A) AST and (B) ALT activities in the sera of chemicals treated mice. Each value represents the mean±SD. *$p<0.05$, **$p<0.01$, vs. control, and +$p<0.05$, vs. CCl_4.

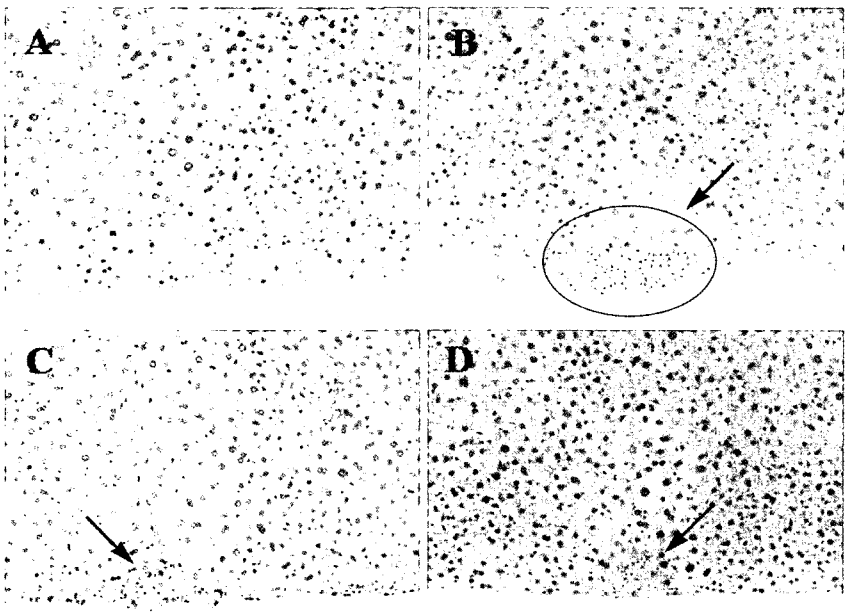

Fig. 2. H&E stained liver sections from mice liver at 24 hr after chemicals treatment. (×200) (A) Control (B) $GdCl_3$ (C) $GdCl_3$+CCl_4 (D) CCl_4.

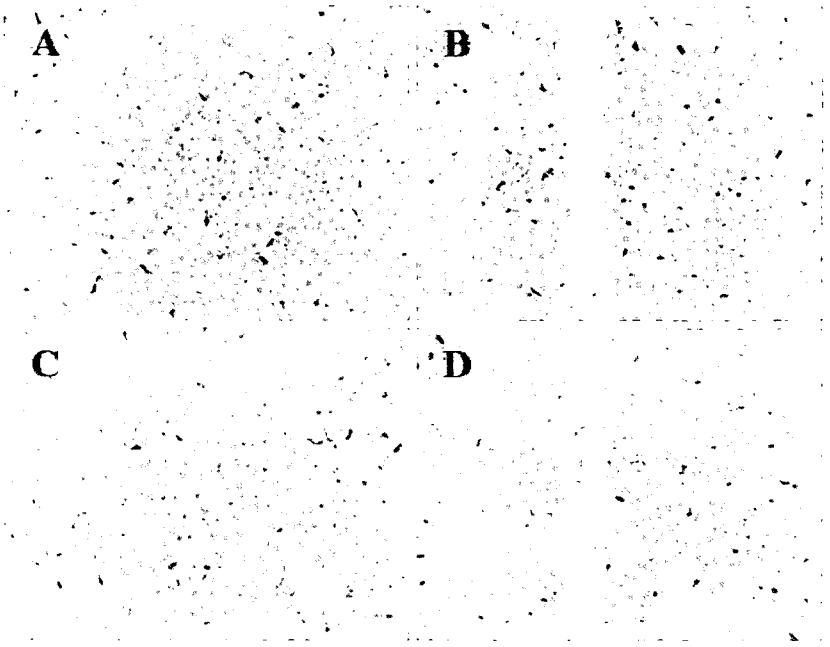

Fig. 3. Evaluation of phagocytotic activity after $GdCl_3$ treatment. (A) Control (B) $GdCl_3$ 10 mg/kg (C) $GdCl_3$ 20 mg/kg (D) $GdCl_3$ 30 mg/kg.

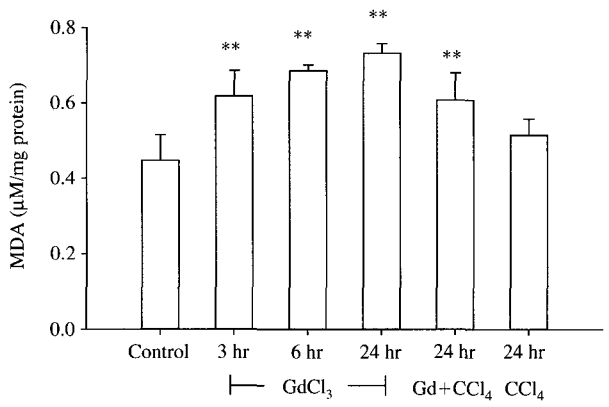

Fig. 4. Malondialdehyde (MDA) content from liver homogenates. Each value represents the mean ± SD. $^{**}p < 0.01$, vs. control.

centration compared to control group (Fig. 3).

Lipid peroxidation is a well-known mechanism of CCl_4-induced liver injury, and MDA is one of its end products[2-4]. Thus, MDA is a good indicator of the severity of lipid peroxidation. Unlike our expectation, treatment with CCl_4 didn't cause an increase of MDA level. Although, treatment with $GdCl_3$ induced significantly in MDA level (Fig. 4).

In this experimental model, $GdCl_3$ didn't inhibit phagocytotic activity and didn't also prevent CCl_4-induced toxicity except biochemical data. Thus, we progressed an experiment to understand effects of $GdCl_3$ on liver by using microarray technique.

Fig. 5. Genetree image gained through hierarchical clustering. Genes were selected through one way ANOVA ($p < 0.05$) considering time parameters as described in methods.

Table 1. Significantly up and down regulated genes by $GdCl_3$ treatment ($p < 0.05$).

Genebank ID	3 hr	6 hr	24 hr	Name	Title
Extracellular matrix					
NM_053192	0.12	0.14	0.22	Uccl	Ependymin related protein 1 (zebrafish)
NM_010577	0.19	0.25	0.34	Itga5	Integrin alpha 5 (fibronectin receptor alpha)
NM_008438	0.34	0.36	0.59	Kera	Keratocan
NM_008605	2.87	8.54	5.8	Mmp12	Matrix metalloproteinase 12
NM_010809	0.25	0.21	0.44	Mmp3	Matrix metalloproteinase 3
NM_015784	2.12	1.48	0.8	Postn	Periostin, osteoblast specific factor
NM_007743	1.83	2.05	4.22	Col1a2	Procollagen, type I, alpha 2
NM_007737	1.38	1.9	3.13	Col5a2	Procollagen, type V, alpha 2
BC005491	2.22	2.94	1.86	Col6a3	Procollagen, type VI, alpha 3
NM_007731	2.38	2.27	1.24	Col13a1	Procollagen, type XIII, alpha 1
NM_009262	2.13	1.8	1.84	Spock1	Sparc/osteonectin, proteoglycan 1
NM_011593	2.47	3.36	2.29	Timp1	Tissue inhibitor of metalloproteinase 1
Cytoskeleton organizatin and biogenesis					
BC003232	2.32	1.58	1.06	Actn1	Actinin, alpha 1
NM_007678	2.29	2.34	1.45	Cebpa	CCAAT/enhancer binding protein, alpha
NM_019682	1.72	1.64	2.42	Dnclc1	Dynein, cytoplasmic, light chain 1
J03458	0.17	0.14	0.17	Flg	Filaggrin
BC003325	0.1	0.11	0.27	Krt1-14	Keratin complex 1, acidic, gene 14
NM_019962	0.19	0.21	0.6	Kif21b	Kinesin family member 21B
NM_008442	0.08	0.1	0.11	Kif2a	Kinesin family member 2A
NM_052976	0.11	0.1	0.17	Ophn1	Oligophrenin 1
NM_011521	2.04	1.84	1.18	Sdc4	Syndecan 4
NM_016667	0.29	1.86	1.68	Sntb1	Syntrophin, basic 1
NM_011526	2.38	1.47	1.57	Tagln	Transgelin
Cell adhesion molecule activity					
NM_007663	2.05	1.38	1.53	Cdh16	Cadherin 16
NM_007643	2.12	1.39	1.07	Cd36	CD36 antigen
NM_017383	0.13	0.13	0.13	Cntn6	Contactin 6
NM_018762	2.27	1.56	1.58	Gp9	Glycoprotein 9 (platelet)
NM_008737	2.01	2.44	1.08	Nrp1	Neuropilin 1
Cytokines related gene/Cytokine receptors					
NM_009757	0.34	0.27	0.37	Bmp15	Bone morphogenetic protein 15
NM_011333	6.28	6.28	6.6	Ccl2	Chemokine (C-C motif) ligand 2
NM_019577	2.43	2.92	1.46	Ccl24	Chemokine (C-C motif) ligand 24
NM_009914	0.18	0.15	0.52	Ccr3	Chemokine (C-C motif) receptor 3
NM_008176	8.41	6.26	1.06	Cxcl1	Chemokine (C-X-C motif) ligand 1
NM_021274	2.1	1.82	1.47	Cxcl10	Chemokine (C-X-C motif) ligand 10
NM_019932	2.57	3.84	4.53	Cxcl4	Chemokine (C-X-C motif) ligand 4
AK013765	0.79	0.48	1.4	Ecgf1	Endothelial cell growth factor 1 (platelet-derived)
NM_020013	4.44	3.97	2.13	Fgf21	Fibroblast growth factor 21
NM_008109	0.23	0.23	0.56	Gdf5	Growth differentiation factor 5
NM_008380	1.19	1.49	2.81	Inhba	Inhibin beta-A
NM_010560	1.48	1.37	2.02	Il6st	Interleukin 6 signal transducer
AK003861	2.14	1.89	1.38	Tgfbr2	Transforming growth factor, beta receptor II
NM_009403	0.07	0.09	0.17	Tnfsf8	Tumor necrosis factor (ligand) superfamily, member 8
Lipid metabolism					
NM_134066	0.11	0.12	0.23	Akr1c18	Aldo-keto reductase family 1, member C18
NM_016668	0.16	0.15	0.63	Bhmt	Betaine-homocysteine methyltransferase
BC003954	2.01	1.99	1.18	Cyp4f13	Cytochrome P450, family 4, subfamily f, polypeptide 13

Table 1. Continued.

Genebank ID	3 hr	6 hr	24 hr	Name	Title
NM_010046	0.19	0.15	0.17	Dgat1	Diacylglycerol O-acyltransferase 1
AK016135	0.28	0.3	0.52	Etnk1	Ethanolamine kinase 1
X13135	1.13	1.24	2.31	Fasn	Fatty acid synthase
NM_033134	1.29	0.93	0.26	Inpp5e	Inositol polyphosphate-5-phosphatase E
AF209926	1.08	1.45	2.2	Icmt	Isoprenylcysteine carboxyl methyltransferase
D26047	0.4	0.34	0.54	Piga	Phosphatidylinositol glycan, class A
NM_008969	2.01	1.48	0.89	Ptgs1	Prostaglandin-endoperoxide synthase 1
NM_011315	2.05	1.43	1.47	Saa3	Serum amyloid A 3
AB016248	0.49	0.39	1.1	Sc5d	Sterol-C5-desaturase homolog (S. cerevisae)
NM_011674	0.32	0.31	0.47	Ugt8	UDP glucuronosyltransferase 8
Oxidative stress					
NM_013602	3.32	6.36	0.57	Mt1	Metallothionein 1
NM_013603	0.97	7.36	0.96	Mt3	Metallothionein 3
Cell death					
NM_013479	0.14	0.16	0.28	Bcl2l10	Bcl2-like 10
NM_007610	0.28	1.4	1.42	Casp2	Caspase 2
AK013476	0.2	0.14	0.25	Faim2	Fas apoptotic inhibitory molecule 2
NM_010370	0.22	0.18	0.18	Gzma	Granzyme A
NM_008655	2.03	2.06	1.78	Gadd45b	Growth arrest and DNA-damage-inducible 45 beta
NM_008109	0.23	0.23	0.56	Gdf5	Growth differentiation factor 5
NM_021451	0.15	0.14	0.18	Pmaip1	Phorbol-12-myristate-13-acetate-induced protein 1
NM_009403	0.07	0.09	0.17	Tnfsf8	Tumor necrosis factor (ligand) superfamily, member 8
NM_011785	1.88	2.21	1.29	Akt3	Thymoma viral proto-oncogene 3
Defense immunity protein activity					
NM_009841	2.98	4.28	3.44	Cd14	CD14 antigen
NM_007643	2.12	1.39	1.07	Cd36	CD36 antigen
NM_007653	2.31	2.6	3.13	Cd63	Cd63 antigen
NM_007851	0.12	0.17	0.29	Defcr5	Defensin related cryptdin 5
AK021160	0.35	0.35	0.73	Lba1	Lupus brain antigen 1
NM_008479	0.28	0.27	0.62	Lag3	Lymphocyte-activation gene 3
AK014535	2.13	1.33	1.08	Sema3d	Sema domain, immunoglobulin domain (Ig)
NM_032542	0.14	0.25	0.36	Sval2	Seminal vesicle antigen-like 2
NM_020047	2.54	1.55	1.23	Tacstd2	Tumor-associated calcium signal transducer 2

Note: Genes presented in shadows were described in this

Gene Expression Analysis

To visualize gene expression change at each time points after treatment with $GdCl_3$, Genetree image gained through hierarchical clustering was shown at Fig. 5. Gene expression pattern among groups were almost similar. However, 24 hr group showed a little different pattern compared to the others. This result coincided with biochemical results that the level of aminotransferase recovered at 24 hr. As described previously, 452 changed genes more than 2 fold in at least one time point was selected and classified by function (Table 1). These selected genes were also subjected to Kyoto Encyclopedia of Genes and Genomes (KEGG) pathway analysis.

As shown at Table 1, extracellular matrix (ECM) and cytoskeleton organization/biogenesis related genes were changed. Though, the reasons for this result were not known, $GdCl_3$-induced toxicity seem to activate stellate cells. These cells which are normally quiescent, on activation, produce ECM including collagens type I and III, and then, this promotes fibrosis. In current study, several types of pro-collagens (Col1a2, Col5a2, Col6a3, and Col13a1) and tissue inhibitor of metalloproteinase1 (TIMP1) were up-regulated during all the time points. An increase of TIMP1 led a diminishment of protease activity, and therefore caused to more matrix accumulation[9]. This matrix accumulation reflects changes in ECM degradation as well as synthesis. In other words, an overall increase of ECM accompanied by a shift from

the normal low density basement membrane like matrix containing non-fibrilforming collagens (i.e. types IV and VI) to one rich in fibril-forming collagens (i.e. types I and III). In present study, matrix metalloproteinase 3 (Mmp3, also called 'stromelysin or transin') was decreased but matrix metalloproteinase 12 (Mmp12, also called 'elastase') was increased. Function of these two enzymes degraded basement membrane collagen (non-fibrilforming) type IV. Contradict, it is reported that Mmp3 also decreased production of fibril forming collagens type III[10]. In previous study, TIMP1 and Mmp12 that were both up-regulated, were identified as fibrosis-specific genes[11].

Effects of ECM are largely mediated by signaling through cell membrane receptors. Integrins are dynamic cell surface receptors that provide a physical link between the extracellular matrix and the cell cytoskeleton[12]. Integrin expression is modified at early stages during liver fibrosis[13].

Fibrogenesis is under the control of several growth factors, chemokines, products of oxidative stress and other soluble factors[14]. TGF-β, primarily a fibrogenic cytokine, is known to play a key role in the fibrogenic response of stellate cell[15]. TGF-β1 can activate hepatic stellate cell and enhance the production of inhibitors of ECM degrading enzymes[16]. At 6 hr after treatment, TGF-β1 was 1.7 fold increased (data not shown). Other growth factor, fibroblast growth factor (FGF) also required for the development of fibrosis[17] and it is coincided with our result that this gene was up regulated during all the time points. Several chemokine ligands (CCL2, CCL24, CXCL1, CXCL4, CXCL10) were up regulated. These chemokines contribute to the formation of the inflammatory infiltration. Fibrosis is close relationship with inflammation[18]. Among them, Chemokine ligand 2 (CCL2, also called 'MCP-1'), a chemoattractant and activator for circulating monocytes and T lymphocytes, was increased during active hepatic fibrogenesis[19].

$GdCl_3$-induced toxicity considered to link to oxidative stress. Several hepatic fibrosis models were accompanied with oxidative stress[20]. Our model, metallothioneins (Mt1 and Mt3), a gene known to play protective roles to oxidative stress, were highly expressed. Further, an increase of lipid peroxidation products (MDA) can be clear evidence as oxidative stress marker. As a mechanism of MDA production, prostaglandin H2 (PGH2) can be breakdown to MDA. PGH2 synthesis catalyzed by prostaglandin endoperoxide H synthases (Ptgs, also called 'cyclooxygenases'). It is reported, under oxidative stress, MDA in plasma partially inhibited by inhibitors of this enzyme[21]. In current study, prostaglandin endoperoxide synthase 1 was up-regulated and thus suspected to induce MDA production.

$GdCl_3$ led abnormality between lipid synthesis and degradation. Fatty acid synthase (Fasn) was up regulated. It is expected to increase fatty acid that can be a substrate for prostaglandin or MDA productions. On the other hand, most of gene related to lipid synthesis as follows down-regulated; Diacylglycerol O-acyltransferase 1 (Dgat1)-catalyzes the terminal step in triacylglycerol synthesis. Ethanolamine kinase 1 (Etnk1)-functions in the first committed step of the phosphatidylethanolamine (one of major class of phospholipids) synthesis pathway. UDP glucuronosyltransferase 8 (Ugt8)-catalyzes the synthesis of galactocerebroside (one of a subclass of sphingolipid). phosphatidylinositol glycan class A (Piga)-takes part in the synthesis of the first intermediate in the biosynthetic pathway of GPI anchor. Sterol-C5-desaturase (Sc5d)-is a critical enzyme in cholesterol synthesis, catalyzing the conversion of lathosterol into 7-dehydrocholesterol[22-25].

Discussion

In conclusion, $GdCl_3$ demonstrated to cause a typical fibrogenesis. This metal changed genes inducing ECM accumulation and encoding several cytokines influenced on fibrosis. $GdCl_3$-induced fibrosis was considered to accompany with inflammation and oxidative stress. Genes related lipid homeostasis was affected, as well. For this study, the application of cDNA microarray technique provided as a powerful tool in identifying and characterizing changes in gene expression associated with toxicity.

Methods

Animal Treatment

Specific pathogen-free male balb/c (11 weeks old) mice were used and acclimated for a week to a 12 hr light/dark cycle in a humidity and temperature-controlled, pathogen-free environment. Five animals per each group were selected. In group 1, $GdCl_3$ was injected (30 mg/kg in saline, i.p.) to cause inactivation of Kupffer cells and then after 24 hr, corn oil was administered. In group 2, $GdCl_3$ was injected, in the same amount as in group 1 and was treated with CCl_4 (0.007 mg/ml in corn oil, i.p.) after 24 hr. In group 3, animals received saline and after 24 hr, CCl_4 was injected. In group 4, control animals received saline and after 24 hr, corn oil. All mice were sacrificed by anesthetizing diethyl ester after 3 hr, 6 hr and 24 hr

after administration. Liver tissues were immediately harvested and submerged in an appreciate volume of RNA*later* (Qiagen, U.S.A.). Liver samples in RNA-*later* were kept at 4°C for overnight and then discarded the reagent, and kept at −80°C until further processing.

Assessment of Liver Injury

Hepatotoxicity was assessed using both biochemical and histological technique. Blood samples drawn from caudal *vena cava* were used to measure AST (asparatate amino transferase), ALT (alanine amino transferase) activity which is indicative of parenchymal cell damage using Fuji Automated Clinical Chemistry Analyzer (Fujifilm, Japan). Liver sections taken at the same time as blood collections were fixed in 10% neutrally buffered formalin and paraffin embedded. Deparaffinized sections (4 μm) were stained with hematoxylin and eosin (H&E), and analyzed by light microscopy.

Evaluation of Phagocytotic Function

$GdCl_3$ was injected (10, 20, 30 mg/kg in saline, i.v.) 1 day prior to 10% Pilot ink (or saline) treatment (10 ml/kg, i.v.). After 4 hr, the livers were removed and stained with H&E.

Malondialdehyde (MDA) Content

Lipid peroxidation was measured using the MDA-586 assay system (OxisResearch™, U.S.A) according to the manufacturer's instructions. Briefly, livers were homogenized in ice-cold 20 mM Tris-HCl (pH 7.4) containing BHT. After centrifuging, protein contents were determined using the Biorad protein assay system (Bio Rad, U.S.A). A 200 μL quantity of sample was assayed for MDA and absorbance was measured at 586 nm.

RNA Extraction

Livers were homogenized in TRI reagent (Molecular Research Center, Inc., U.S.A) for RNA isolation. Total RNA was further purified using the RNeasy Mini Kit (Qiagen, U.S.A.). Final products yielded 260/280 nm ratios of 1.8-2.1, 230/260 nm ratio >2.0. RNA quality was checked by bioanlayzer 2100 (Agilent, U.S.A.).

Microarray Experiments

Mouse Oligo 10 K chips, composed of 9850 known genes, were purchased from Genomic Tree Inc., Korea. Microarray experiments were performed according to the manufacturer's standard protocol. Briefly, the RNA from the 5 mice in control group was pooled using equal amounts from each mouse to make a total of 100 μg of RNA and the RNA from the 3 mice in treatment group was individually prepared.

These sample was labeled with Cy3 (for control) or Cy5 (for treatment) dye coupling with dUTP by a reverse-transcription reaction using reverse transcriptase and the oligo (dT) primer. The fluorescently labeled cDNAs were mixed and hybridized to the oligo chip. After the washing procedure, the DNA chips were scanned using GenePix 4000B (Axon Instrument, Inc., U.S.A.).

Data Analysis

Data analyses were performed using the GeneSpring 7.2 (Silicon Genetics, U.S.A.). To generate the relative intensity (ratio) value, each gene's measured intensity was divided by its control value in each sample. To correct for dye-related artifacts resulting from nonlinear rates of dye incorporation and inconsistencies in the relative fluorescence intensity between the red and green dyes, we used an intensity-dependent LOWESS normalization. Then data were filtered using the control signal, a control value calculated using the Cross-Gene Error Model based on replicates. Genes with higher control signal are relatively more precise than genes with lower control signal. Genes that didn't reach this value were discarded. To identify differentially expressed genes, all genes are filtered on t test $p<0.05$ using Filtering on Confidence. And then, we selected up or down regulated genes more than 2 fold changes in at least one time point. We used hierarchical clustering algorithms to divide genes into groups that have similar expression patterns considering time parameters (ANOVA, $p<0.05$). The GenBank accession number and the full annotation gene name for each gene were incorporated and classified by function. KEGG map analysis enabled visualization of gene expression by microarray data on maps representing biological pathways and groupings of genes (http://www.genome.jp/kegg/).

Statistical Data Analysis

Significant differences to the controls were calculated using one way ANOVA with post test (Dunnett Multiple Comparisons Test). To compare statistical significance between two groups, two-tailed, unpaired t test was performed.

Acknowledgements

This work was supported by the Ministry of Science and Technology for the 2005 Advanced Project for an International Accreditation of the Preclinical Sa-

fety Evaluation System for Korea Institute of Toxicology.

Reference

1. Hustzik, E., Lazar, G. & Parduez, A. Electron microscopic study of Kupffer-cell phagocytosis blockade induced by gadolinium chloride. *Br. J. Exp. Pathol.* **61**, 624-630 (1980).
2. Muriel, P. *et al.* Kupffer cells inhibition prevents hepatic lipid peroxidation and damage induced by carbon tetrachloride. *Comp. Biochem. Physiol.* **130**, 219-226 (2001).
3. Muriel, P. & Escobar, Y. Kupffer cells are responsible for liver cirrhosis induced by carbon tetrachloride. *J. Appl. Toxicol.* **23**, 103-108 (2003).
4. Giakoustidis, D.E. *et al.* Blockade of Kupffer cells by gadolinium chloride reduces lipid peroxidation and protects liver from ischemia/reperfusion injury. *Hepatogastroenterology* **50**, 1587-1592 (2003).
5. Rivera, C.A. *et al.* Attenuation of CCl_4-induced hepatic fibrosis by $GdCl_3$ treatment or dietary glycine. Am. J. Physiol. Gastrointest. *Liver Physiol.* **281**, 200-207 (2001).
6. Cynthia, J. *et al.* Protective Role of Kupffer Cells in Acetaminophen-Induced Hepatic Injury in Mice. *Chem. Res. Toxicol.* **15**, 1504-1513 (2002).
7. Spencer, A., Wilson, S. & Harpur, E. Gadolinium chloride toxicity in the mouse. *Hum. Exp. Toxicol.* **17**, 633-637 (1998).
8. Wroblewski, F. The clinical significance of alterations in transaminase activities of serum and other body fluids. *Adv. Clin. Chem.* **1**, 313-351 (1958).
9. Iredale, J.P. *et al.* Tissue inhibitor of metalloproteinase-1 messenger RNA expression is enhanced relative to interstitial collagenase messenger RNA in experimental liver injury and fibrosis. *Hepatology* **24**, 176-184 (1996).
10. Sansilvestri-Morel, P. *et al.* Decreased production of collagen Type III in cultured smooth muscle cells from varicose vein patients is due to a degradation by MMPs: possible implication of MMP-3. *J. Vasc. Res.* **42**, 388-398 (2005).
11. Chung, H. *et al.* Differential gene expression profiles in the steatosis/fibrosis model of rat liver by chronic administration of carbon tetrachloride. *Toxicol. Appl. Pharmacol.* **208**, 242-254 (2005).
12. Dedhar, S. Integrins and signal transduction. *Curr. Opin. Hematol.* **6**, 37-43 (1999).
13. Scoazec, J.Y. Expression of cell-matrix adhesion molecules in the liver and their modulation during fibrosis. *J. Hepatol.* **22**(Suppl), 20-27 (1995).
14. Olaso, E. & Friedman, S.L. Molecular regulation of hepatic fibrogenesis. *J. Hepatol.* **29**, 836-847 (1998).
15. Tahashi, Y. *et al.* Differential regulation of TGF-beta signal in hepatic stellate cells between acute and chronic rat liver injury. *Hepatology* **35**, 49-61 (2002).
16. Ma, C., Tarnuzzer, R.W. & Chegini, N. Expression of matrix metalloproteinases and tissue inhibitor of matrix metalloproteinases in mesothelial cells and their regulation by transforming growth factor-beta1. *Wound Repair Regen.* **7**, 477-485 (1999).
17. Yu, C. *et al.* Role of fibroblast growth factor type 1 and 2 in carbon tetrachloride-induced hepatic injury and fibrogenesis. *Am. J. Pathol.* **163**, 1653-1662 (2003).
18. Ramadori, G., Knittel, T. & Saile, B. Fibrosis and altered matrix synthesis. *Digestion* **59**, 372-375 (1998).
19. Marra, F., DeFranco, R., Grappone, C. & Abboud, H.E. Increased expression of monocyte chemotactic protein-1 during active hepatic fibrogenesis: correlation with monocyte infiltration Am. *J. Pathol.* **152**, 423-430 (1998).
20. Poli, G. Pathogenesis of liver fibrosis: role of oxidative stress. *Mol. Aspects. Med.* **21**, 49-98 (2000).
21. Kadiiska, M.B. *et al.* Biomarkers of oxidative stress study III. Effects of the nonsteroidal anti-inflammatory agents indomethacin and meclofenamic acid on measurements of oxidative products of lipids in CCl_4 poisoning. *Free. Radic. Biol. Med.* **38**, 711-718 (2005).
22. Rustan, A.C., Nossen, J.O., Christiansen, E.N. & Drevon, C.A. Eicosapentaenoic acid reduces hepatic synthesis and secretion of triacylglycerol by decreasing the activity of acyl-coenzyme A: 1, 2-diacylglycerol acyltransferase. *J. Lipid. Res.* **29**, 1417-1426 (1988).
23. Kim, K., Kim, K.H., Storey, M.K., Voelker, D.R. & Carman, G.M. Isolation and characterization of the Saccharomyces cerevisiae EKI1 gene encoding ethanolamine kinase. *J. Biol. Chem.* **274**, 14857-14866 (1999).
24. Miyata, T. *et al.* The cloning of PIG-A, a component in the early step of GPI-anchor biosynthesis. *Science* **259**, 1318-1320 (1993).
25. Sugawara, T., Fujimoto, Y. & Ishibashi, T. Molecular cloning and structural analysis of human sterol C5 desaturase. *Biochim. Biophys. Acta.* **1533**, 277-284 (2001).